# High-Conversion Catalytic Chain Transfer Polymerization of Methyl Methacrylate

**S. C. J. Pierik, A. M. van Herk**

*Laboratory of Polymer Chemistry, Eindhoven University of Technology, P. O. Box 513, 5600 MB Eindhoven, The Netherlands*

Received 7 November 2002; accepted 24 February 2003

**ABSTRACT:** In this work the effects of conversion on the apparent catalyst activity in the catalytic chain transfer polymerization of methyl methacrylate are reported. Several mechanisms are discussed that may explain the experimental observations. The discussion is supported with computer simulations using Predici software. It is shown that the experimental decrease in weight average molecular weight with conversion is smaller than the decrease obtained in simulations. The most likely cause for this discrepancy is slow catalyst deactivation. The half-life of CoBF under the reported conditions was determined to be about 10 h. Furthermore, the effect of acetic acid (HAc) and benzoyl peroxide (BPO) on the evolution of the molecular weight distribution is investigated. Both HAc and BPO enhance catalyst deactivation. For HAc, catalyst deactivation scales with the square root of its concentration. BPO- enhanced deactivation depends linearly on its concentration. © 2003 Wiley Periodicals, Inc. J Appl Polym Sci 91: 1375–1388, 2004

**Key words:** radical polymerization; macromonomers; catalytic chain transfer; kinetics (polym.)

## INTRODUCTION

In the past two decades catalytic chain transfer (CCT) has emerged as a useful, industrial applicable technique to prepare low molecular weight macromonomers.[1–3] The catalyst is usually a low-spin Co(II) species able to catalyze the chain transfer to monomer reaction in the free-radical homopolymerization[4–6] of methacrylates, $\alpha$-methylstyrene, and styrenes, and in the copolymerization with other monomers like acrylates.[7] Cobaloxime boron fluoride (CoBF), presented in Figure 1, is a typical example of a highly active CCT catalyst that is frequently used in academic studies. The generally accepted mechanism for CCT consists of two consecutive reactions as shown for methyl methacrylate (MMA) in Figure 2. In the first step the Co(II) species abstracts hydrogen from the growing polymer chain resulting in the formation of a cobalt hydride and a macromonomer. In the second step the cobalt hydride reacts with monomer to reinitiate a new growing chain, thereby regenerating the initial Co(II) species. The Mayo equation can be used to determine the chain transfer constant ($C_T$) for this process:

$$\frac{1}{P_n} = \frac{1}{P_{n0}} + C_T \frac{[\mathrm{Co(II)}]}{[\mathrm{M}]} \quad (1)$$

in which $P_n$ is the number average degree of polymerization, $P_{n0}$ is the number average degree of polymerization without transfer agent present, [Co(II)] and [M] are the concentrations of cobalt- species and monomer, respectively. $C_T$ is the ratio of $k_{tr}$ and $k_p$, which are the rate coefficients of transfer and propagation, respectively. In four reviews many aspects of CCT have been discussed.[8–11]

Most kinetic studies on catalytic chain transfer polymerization are focused on low-conversion polymerizations. For practical applications, on the other hand, it is very important and interesting to study these polymerizations up to high conversions. From literature, some studies aiming at the production of larger amounts of macromers are known. Suddaby et al.[12] described a continuous process for the production of macromers in a tubular reactor. A similar setup was applied by Grady.[13] However, steady state conversion only reached 14% and mean residence times were below 25 min. So, although continuous operation can be a good alternative, it does not resemble high-conversion batch reactions and cannot be used as a point of reference. Some other studies were mainly focused on the production of dimer at high catalyst concentrations and subsequent copolymerization with other monomers.[14,15] Most kinetic studies were carried out in the group of Davis and Heuts.[16–22] For nearly all studies molecular weight distributions did not or hardly change with conversion, whereas a decrease, which would be expected according to the Mayo equation (1), was only observed experimentally by Kowollik et al.[20] Several explanations have been suggested

*Correspondence to:* A. M. van Herk (A.M.v.Herk@tue.nl).

Journal of Applied Polymer Science, Vol. 91, 1375–1388 (2004)

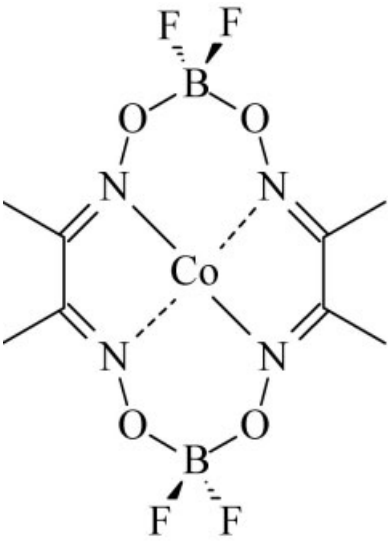

**Figure 1** Structure of CoBF.

like catalyst deactivation and catalyst–solvent interactions that change with conversion and compensate for a decrease in monomer concentration. In this article various mechanisms will be discussed and related to new experiments as well as Predici simulations in order to find an explanation for the discrepancy between the predictions according to the Mayo equation and most experimental results. Furthermore, it will be investigated whether added contaminants like acetic acid and benzoyl peroxide affect the evolution of the molecular weight distribution in high-conversion polymerizations.

All investigations in this work are based on observations of the polymerization kinetics combined with Predici computer simulations. An alternative or complementary approach could be to directly monitor the Co(II) concentration. Although some reports are known in which the concentration of cobalt catalyst was followed by electron spin resonance (ESR) measurements,[17] it is very difficult to measure Co(II) concentration in a polymerizing system by ESR or any other technique, due to the very small amounts of cobalt complex present. Therefore, it was chosen to focus on polymerization kinetics in the investigation of CCT polymerizations up to high conversion.

## EXPERIMENTAL

### Materials

Methyl methacrylate (MMA, Merck, 99%) (The Netherlands) was distilled under vacuum, and stored at −10°C. Prior to use, MMA was passed over a column, containing inhibitor remover and basic alumina. Toluene (Biosolve, AR) (The Netherlands) was purified using a Grubbs solvent setup,[23] purged with argon for at least 3 h, and stored over molsieves in a glovebox. Azobis(methylisobutyrate) (AIBMe, Wako Chemicals, Germany) was recrystallized once from methanol and stored in a glovebox. Benzoyl peroxide (Aldrich, 97%) (The Netherlands) and acetic acid (Merck, 99%) were used as received.

CoBF [bis(aqua)bis((difluoroboryl)dimethylglyoximato)cobalt(II)] was prepared according to a procedure of Bakac and Espenson.[24] One batch was used throughout all experiments. It was analyzed using ultraviolet-visible (UV-Vis) spectroscopy and elemental analysis (experimental: C: 22.9%, H: 3.79%, N: 13.2%; calculated for $C_8H_{12}N_4O_4B_2F_4Co \cdot (H_2O)_2$: C: 22.8%, H: 3.83%, N: 13.3%).

### General polymerization procedure

Monomer and solvent were purged with argon for at least 3 h prior to transfer into a glovebox. All reaction mixtures were prepared inside a glovebox. Stock solutions of CoBF in monomer or solvent were prepared and stored for a longer period of time. AIBMe solutions in monomer were prepared immediately prior to the experiment. Reaction mixtures were made of the CoBF solution, monomer, toluene, and an AIBMe solution to a total volume of about 50 mL in a three-necked round-bottom flask. Polymerizations were carried out in a sand bath at a constant temperature of 60°C (±1.5°C). A thermocouple was immersed into the reaction mixture for optimal control. The mixtures were stirred with a magnetic stirrer. Polymerizations were carried out inside a glovebox to prevent oxygen from entering the reaction mixture during sampling. Samples were withdrawn by syringe to monitor conversion and molecular weight distribution. Reactions were stopped by addition of hydroquinone and cooling. Monomer was evaporated at room temperature and the polymer dried under vacuum at 60°C. Conversion was determined gravimetrically. An overview of experimental conditions for all eight experiments is presented in Table I.

### Analyses

Size exclusion chromatography (SEC) was carried out using tetrahydrofuran (THF) as an eluent at a flow rate of 1 mL×min$^{-1}$. Two Polymer Laboratories PLgel

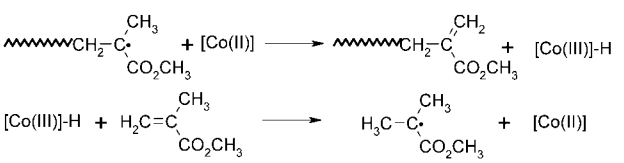

**Figure 2** Mechanism of catalytic chain transfer steps in the polymerization of MMA.

**TABLE I**
**Overview of Experimental Conditions for High-Conversion CCT Polymerizations**

| Experiment | $w_{MMA}$ (—) | [CoBF] ($10^{-6}$ mol · $L^{-1}$) | Additive | [Add.] (mol · $L^{-1}$) |
|---|---|---|---|---|
| I | 1 | 9.1 | — | — |
| II | 0.42 | 3.0 | — | — |
| III | 0.42 | 1.0 | — | — |
| IV | 0.17 | 1.0 | — | — |
| V | 0.42 | 3.0 | HAc | 0.10 |
| VI | 0.42 | 3.0 | HAc | 1.0 |
| VII | 0.42 | 3.0 | BPO | $1.0 \times 10^{-3}$ |
| VIII | 0.42 | 3.0 | BPO | $4.0 \times 10^{-3}$ |

5 $\mu$m Mixed-C columns (300 × 7.5 mm) and PLgel 5 $\mu$m guard column (50 × 7.5 mm) were used and calibrated with Polymer Laboratories narrow MWD polystyrene standards. The Mark–Houwink parameters used in universal calibration are: $K_{MMA} = 9.44 \times 10^{-5}$dL× $g^{-1}$, $a_{MMA} = 0.719$, $K_S = 1.14 \times 10^{-4}$ dL× $g^{-1}$, $a_S = 0.716$.[25]

### Computer simulations

Polymerization kinetics were modeled using the Predici software package, version 5.21.2. This software is especially designed to model polymerizations. The simulations were run on a 233 MHz Intel Pentium computer equipped with 32 MB of RAM and a Windows 98 operating system. Standard simulation settings are chosen and the relative integrator accuracy is set to 0.01. Unless otherwise stated simulations are run in moments mode. The standard set of reactions taken into account in the simulations is shown in Figure 3. The corresponding rate coefficients are either taken from literature[26–28,35] or estimated and presented in Table II.

## RESULTS AND DISCUSSION

### High-conversion CCT polymerizations in bulk and solution

As mentioned in the introduction in most papers published so far about CCT most polymerizations are run up to conversions less than about 5%. At higher conversions and longer reaction times, other factors come into play. Depending on solvent concentration and polymer molecular weight, viscosity increases with conversion. Although the occurrence of diffusion control at low conversions is still debated, it may very well be present at high conversion. Furthermore, as the reactions are carried out over a longer time span, the effects of catalyst deactivation, if present, are more likely to be observable. Another aspect that has to be taken into consideration is that the resulting macromers can, in principle, take part in subsequent reaction steps. In order to get a general idea about the effects of conversion, first two typical high conversion polymerizations will be discussed.

The first experiment (I) is a bulk polymerization of MMA, whereas the second (II) is a solution polymerization in toluene at 41.5% of MMA. At regular time intervals samples were withdrawn and analyzed for conversion and molecular weight distribution. First-order kinetic plots for both polymerizations are shown in Figures 4 and 5. In Figure 6 a typical example of a MWD is presented, in which the areas under the curves are proportional to the conversions determined for the corresponding samples are presented. In Figure 7 the evolution of $M_w$ can be found. $M_w$ is preferred over $M_n$ as it is less sensitive to SEC artifacts.

The first-order kinetic plots shown in Figure 4 and 5 are straight up to high conversions, which means that the radical concentration remains constant. Theoretically the linear fits are expected to go through the origin, but this is not observed. This can be explained by temperature effects, viz. a slight temperature overshoot for experiment I and too slow heating for experiment II.

As can be seen from Figure 7 for both polymerizations, when looking at the whole conversion range, the MWD shifts to lower molecular weights in spite of a slight increase at lower conversions. In a polymerization similar to experiment II, Kukulj et al.[16] obtained slightly increasing molecular weights. Heuts et al.[22] recently also reported a slight decrease in molecular

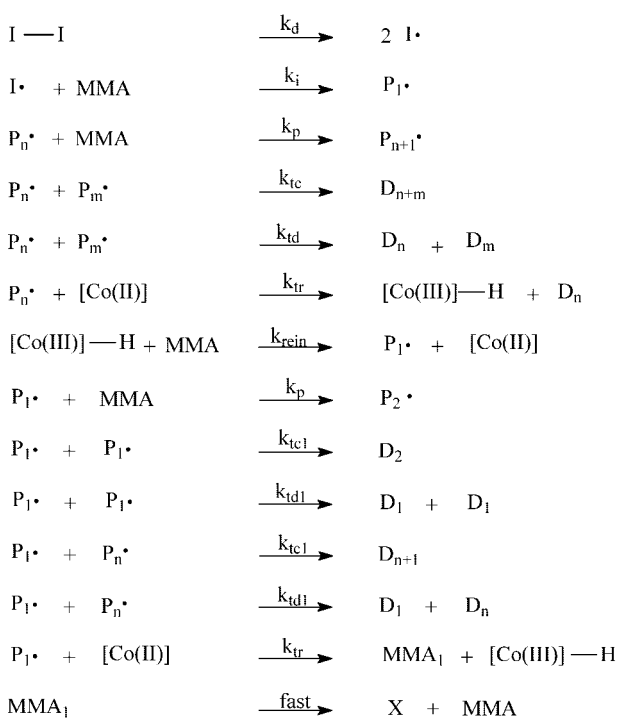


**Figure 3** All reaction steps taken into account in Predici simulations.

**TABLE II**
**Rate Coefficients for the CCT Polymerization of MMA at 60°C Used in Predici Simulations**

| Rate constant | Value | Remarks |
|---|---|---|
| $k_d$ | $9.7 \times 10^{-6}$ s$^{-1}$ | Taken from ref. 34. Initiator efficiency is set to 1 |
| $k_i$ | 2530 L · mol$^{-1}$ · s$^{-1}$ | Recalculated from ref. 26 assuming equal activation energies for initiation and propagation |
| $k_P$ | 833 L · mol$^{-1}$ · s$^{-1}$ | Taken from ref. 27 |
| $k_{tc}$, $k_{td}$ | $5 \times 10^7$ L · mol$^{-1}$ · s$^{-1}$ | Recalculated from ref. 28 |
| $k_{tc1}$, $k_{td1}$ | $1.5 \times 10^8$ L · mol$^{-1}$ · s$^{-1}$ | Estimated |
| $k_{tr}$ | $3.3 \times 10^7$ L · mol$^{-1}$ · s$^{-1}$ | Calculated using $C_T = 39.6 \times 10^3$ |
| $k_{rein}$ | $1 \times 10^3$ L · mol$^{-1}$ · s$^{-1}$ | Estimated |

weight in the terpolymerization of styrene, MMA, and 2-hydroxyethyl methacrylate, but it is very hard to interpret these data in a straightforward way, as the presence of three monomers considerably complicates the system. Kowollik et al.[20] reported an experimentally determined decrease of 45% in $M_w$ going from 10 to 100% conversion. Simulations showed that such a decrease corresponds to what is expected when the Co(II) concentration remains unchanged and monomer is consumed.[20] The decrease in $M_w$ in the experiments presented here is only about 20%. So, it seems that the effect of monomer consumption on $M_w$ is in some way counteracted.

Simulations, similar to those of Kowollik et al,.[20] were performed using the model presented in Figure 3 and Table II to see the effect of conversion on molecular weight. The chain transfer constants for both simulations were calculated from the second sample of the corresponding experiments. In this calculation the term in the Mayo equation expressing the contribution of polymer formed in the absence of chain transfer agent is neglected. This results in $C_T = 40.8 \times 10^3$ for the bulk polymerization and $C_T = 46.1 \times 10^3$ for the solution polymerization. Considering that both are determined from a single point the results are in quite good agreement and compare well with results obtained from low conversion polymerizations.[29]

The simulation results are shown in Figure 7 as well. For the bulk polymerization the general trend in the experimental data and the simulation data is the same. For the solution polymerization at about 25% conversion the experimental data start to deviate from the simulation results. So, the molecular weights produced experimentally do not decrease as much as predicted by model simulations. There can be several general explanations for the discrepancy between the experimental results presented here, on the one hand, and the experimental results of Kowollik et al.[20] and our Predici computer simulations, on the other hand. This can be due to (1) a decrease in intrinsic activity of the catalyst due to changing reaction conditions, (2) a decrease in the concentration of the active form of the catalyst, and (3) additional growth of polymer chains formed at lower conversions. In the next sections all three possibilities will be considered.

### Changes in catalyst activity

Kukulj et al.[16] suggested that the continuously changing ratio of monomer to solvent may be a possible

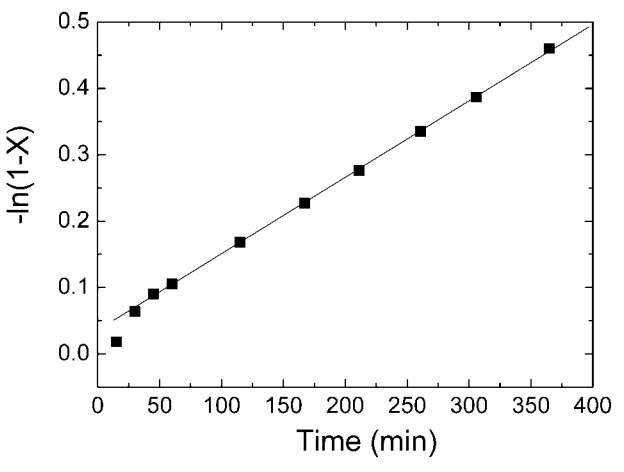


**Figure 4** First-order kinetic plot of the CCT polymerization of MMA in bulk at 60°C.

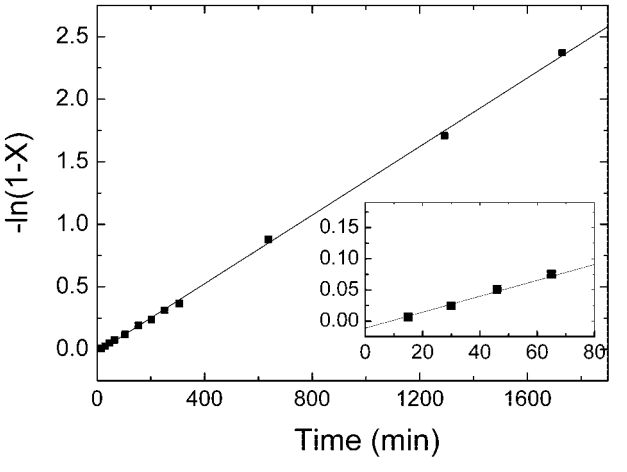


**Figure 5** First-order kinetic plot of the CCT polymerization of MMA in toluene at 60°C. In the insert the first-order kinetic plot at short reaction times is shown.

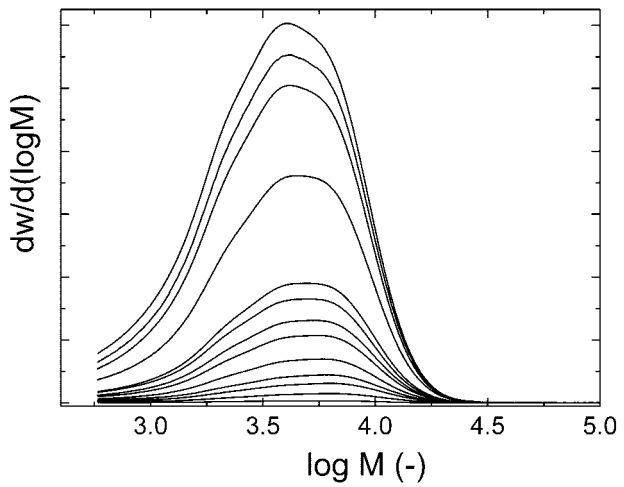


**Figure 6** Typical molecular weight distributions measured at increasing conversions for the CCT polymerization of MMA in toluene at 60°C; $w_{MMA} = 0.419$. The relative areas under the plots correspond to the monomer conversions. Conversions range from 0.6 to 100%.

explanation for decreasing catalyst activity. However, Heuts et al.[18] tested this hypothesis by determining the chain transfer coefficients from experiments at constant catalyst concentrations and varying monomer concentrations and did not obtain any evidence in support of this hypothesis. Results on solvent effects, in which $C_T$ proved to be independent of toluene concentration, as discussed in a previous article[29] point in the same direction. So the explanation that changes in the ratio of monomer concentration and solvent concentration affect $C_T$ can be discarded.

A second possibility is that due to the formation of polymer, the viscosity of the reaction mixture increases. Although in our opinion diffusion control is not expected to play a role at lower conversions, it may affect the catalytic chain transfer step at higher conversions. The molecular weights, however, are not that high and therefore no excessive viscosity increase is expected. When viscosity would affect the chain transfer rate constant, it would most probably also affect the termination rate constants. In that case the first-order kinetic curves shown in Figures 4 and 5 would show an upward deviation from linearity. This is not observed. Furthermore, Heuts[30] reported that adding polymer to a catalytic chain transfer polymerization in order to increase viscosity did not affect the obtained chain transfer coefficients. Therefore, it is expected that at least in these experiments restricted diffusion cannot explain the limited molecular weight shift. In conclusion, the explanation for the development of the MWDs in the CCT polymerizations presented here cannot be found in changes in intrinsic catalytic activity of the chain transfer agent.

### Catalyst deactivation

Catalyst deactivation can proceed via various pathways. Most likely these are spontaneous temperature- or acid-induced decomposition of the catalyst complex, oxidation by oxygen or oxygen-centered radicals, or the formation of thermodynamically or kinetically stable Co(III)-R compounds. However, other deactivation pathways cannot be ruled out at this stage. In order to be able to model deactivation it is useful to obtain experimental plots of the change in concentration of active Co(II) in time. Kukulj et al.[16] carried out similar calculations to calculate the change in $C_T$. Assuming $C_T$ is constant, it is possible to calculate the fraction of active cobalt(II). Kukulj et al. chose to do this via subtraction of the scaled molecular weight distributions. This results in scattered data caused by errors in the subtraction of the low molecular weight tails of the molecular weight distribution. Therefore, it was decided to calculate the fraction of cobalt(II) via the instantaneous weight average molecular weight, $M_{w,\mathrm{in}}$, which can be calculated from the cumulative weight average molecular weight, $M_{w,\mathrm{cum}}$. The $M_w$ of a polymer formed in a time period $\Delta t$ is defined as

$$M_{w,\Delta t} = \frac{\Sigma\, W_{i,\Delta t} M_{i,\Delta t}}{\Sigma\, W_{i,\Delta t}} \qquad (2)$$

in which $W_{i,\Delta\ t}$ is the mass of polymer chains with chain length $i$ formed in time period $\Delta t$ and $M_{i,\Delta\ t}$ is the molecular weight of a chain with length $i$. The nominator can be rewritten as the difference of the sum at time $t+\Delta t$ and the sum at time $t$, whereas the denom-

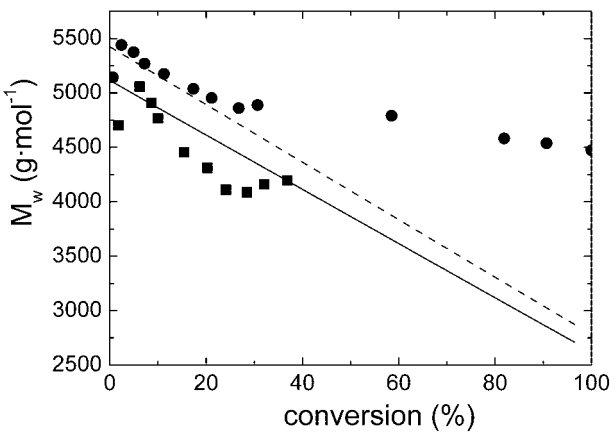


**Figure 7** Evolution of $M_w$ for the CCT polymerization of MMA at 60°C. Solid squares: bulk MMA; solid circles: solution in toluene with $w_{MMA} = 0.415$. The curves are predictions from computer simulations using Predici. The model in Figure 2 was used; $k_{tr}$ was calculated from the second experimental data point. The dashed line represents the solution polymerization, the solid line the bulk polymerization.

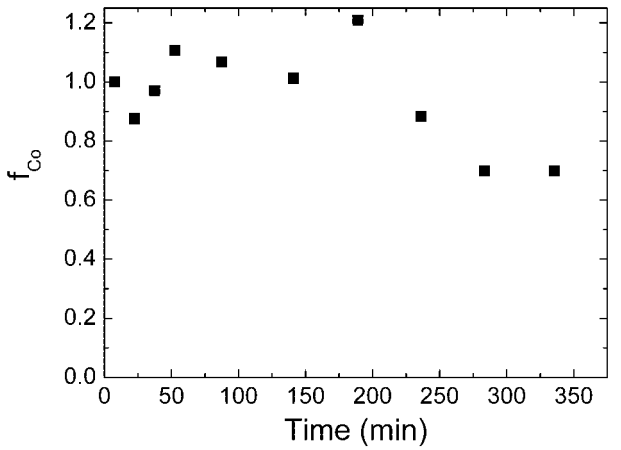


**Figure 8** The evolution of the fraction of cobalt present as Co(II) in the CCT polymerization of MMA in bulk at 60°C (experiment I).

inator can be rewritten as the amount of monomer converted into polymer during time period $\Delta t$, resulting in

$$M_{w,\Delta t} = \frac{\Sigma\, W_{i,t+\Delta t} M_{i,t+\Delta t} - \Sigma\, W_{i,t} M_{i,t}}{m_0 \Delta X} \tag{3}$$

in which $m_0$ is the initial amount of monomer and $\Delta X$ is the conversion in time period $\Delta t$, i.e., $\Delta X = X_{t+\Delta\, t} - X_t$. Both terms in the nominator of eq. (3) can be rewritten as the product of conversion and $M_w$ at their specific times giving

$$M_{w,\Delta t} = \frac{m_0 X_{t+\Delta t} M_{w,t+\Delta t} - m_0 X_t M_{w,t}}{m_0 \Delta X} \tag{4}$$

For a time period $\Delta t$ corresponding to relatively small changes in conversion, $M_{w,\Delta\, t}$ will approximate $M_{w,\mathrm{in}}$ which can be used in the Mayo equation. So

$$M_{w,\mathrm{in}} = \frac{\Delta(X M_{w,\mathrm{cum}})}{\Delta X} \tag{5}$$

Now, it is possible to relate the cobalt(II) concentration at time $t_2$ to the cobalt(II) concentration at time $t_1$ via the respective Mayo equations at those times.

$$\frac{[\mathrm{Co(II)}]_{t_2}}{[\mathrm{Co(II)}]_{t_1}} = \frac{\left(\frac{1}{P_{n,t_2}} - \frac{1}{P_{n,o,t_2}}\right)\frac{[\mathrm{M}]_{t_2}}{C_T}}{\left(\frac{1}{P_{n,t_1}} - \frac{1}{P_{n,o,t_1}}\right)\frac{[\mathrm{M}]_{t_1}}{C_T}} \tag{6}$$

Neglecting the contributions of the inverse degree of polymerization in absence of catalyst and assuming that for the first sample, taken relatively shortly after the start of reaction, the amount of Co(II) still equals the initial amount, this results in

$$f_{\mathrm{Co}} = \frac{(1 - X_{t_2}) P_{n,t_1}}{(1 - X_{t_1}) P_{n,t_2}} \tag{7}$$

In this way the fraction of Co(II) available for chain transfer, $f_{\mathrm{Co}}$, can be estimated from the experimental results. In these calculations average times and conversion are used. In Figures 8 and 9 the results of these calculations are shown for experiments I and II, respectively. As can be seen in Figure 8 especially, the data for $f_{\mathrm{Co}}$ still show some scatter. This is most probably the reason that in some cases $f_{\mathrm{Co}}$ is larger than one, which is of course physically unrealistic, unless the initially added cobalt complex was not completely present as Co(II) and is regenerated during polymerization. So during the first few hours of the reaction the amount of Co(II) is fairly constant, after which deactivation sets in. For the solution polymerization, less than 10% of the initially added amount is still active after about 35 h. A similar trend can be seen in the work of Kukulj et al.[16]

In the beginning of this section a few possible causes for deactivation were mentioned. Oxidation by oxygen is unlikely as all solvents and monomers were freed from oxygen and taken into a glovebox having a nitrogen atmosphere containing less than 1 ppm of oxygen. Furthermore, both reaction mixture preparation and polymerization are performed inside a glovebox. As was shown before,[31] small amounts of oxygen that may still be present in spite of all precautions taken do hardly influence the polymerization. So oxygen is most probably not causing deactivation. The second pathway, spontaneous or acid induced decomposition cannot be excluded beforehand. The third pathway, formation of Co(III)-R compounds, could in

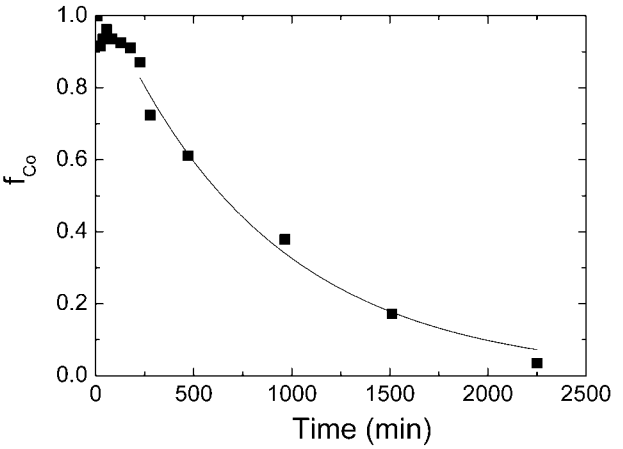


**Figure 9** The evolution of the fraction of cobalt present as Co(II) in the CCT polymerization of MMA in toluene solution at 60°C (experiment II).

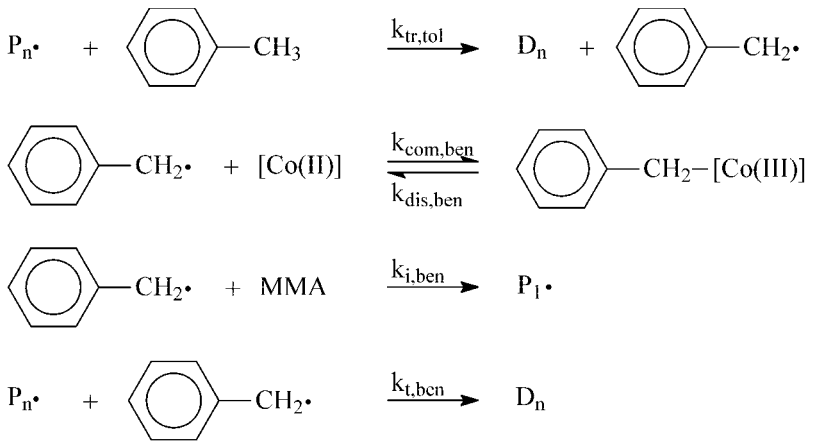


**Figure 10** Co(II) deactivation via solvent-derived radicals.

principle proceed via chain transfer to solvent as shown for toluene in Figure 10. Transfer to solvent results in a radical that can reinitiate or terminate polymerization, but which can also combine with Co(II). This may cause, depending on the rate of transfer to solvent and the dissociation rate of the Co(III)-R compound, a substantial buildup of Co(III), thereby reducing the amount of Co(II). Both spontaneous decomposition and deactivation via solvent-derived radicals will be modeled using Predici. The model presented above is extended with these reactions (see also Fig. 10). Spontaneous decomposition will be assumed to be a first-order process. Reaction rate constants are estimated or taken from literature[24,26,32] and shown in Table III.

The simulation results for deactivation via transfer-derived radicals are shown in Figure 11 together with experimental data for experiment II. Two simulated curves are shown. The solid line represents simulation results according to the data in Table III. The dashed line shows results for stronger Co(III)–benzyl formation, originating from either (1) an increased transfer to toluene rate constant or (2) an increased Co(II)–benzyl combination rate constant or (3) a decreased rate constant for addition of benzyl radicals to MMA. It can be clearly seen that the experimental data and the simulation results do not agree in either case. This does not necessarily mean Co(III)– benzyl formation does not take place but it is clearly not the major or only mechanism responsible for the experimental observations.

In Figure 12 the simulation results for a first order decomposition of the Co(II) complex are shown. Bakac and Espenson[24] report a first order deactivation rate constant of $6.9 \times 10^{-4}$ s$^{-1}$ in a 0.1*M* aqueous solution of $HClO_4$, most probably at ambient temperature. Although the polymerization reaction conditions differ widely from those described in Bakac and Espenson's experiment, a first-order deactivation process with a rate constant of $1 \times 10^{-4}$ s$^{-1}$ seems a good starting point. It can be seen in Figure 12 that a spontaneous decomposition process can provide a better fit to the experimental data than deactivation via transfer derived radicals. Unfortunately, this does not result in any concrete information regarding the mechanism of decomposition.

In summary, it can be said that if catalyst deactivation is the reason for the deviations in $M_w$ between simulations and experiments, spontaneous deactivation is more likely to occur than oxidation by oxygen or formation of stable Co(III)–R compounds.

**TABLE III**
**Additional Rate Coefficients to Be Used in Computer Simulations Using Predici Software**

| Description | Rate constant | Value | Reference/Remarks |
|---|---|---|---|
| Transfer to toluene | $k_{tr,tol}$ | $2.1 \times 10^{-2}$ L · mol$^{-1}$ · s$^{-1}$ | Taken from ref. 32 |
| Initiation of MMA by benzyl radical | $k_{i,ben}$ | $8 \times 10^{3}$ L · mol$^{-1}$ · s$^{-1}$ | Extrapolated from ref. 26 |
| Termination by benzyl radical | $k_{t,ben}$ | $1.5 \times 10^{8}$ L · mol$^{-1}$ · s$^{-1}$ | Estimated |
| Benzyl–Co(III) formation | $k_{com,ben}$ | $6 \times 10^{8}$ L · mol$^{-1}$ · s$^{-1}$ | Extrapolated from ref. 24 |
| Benzyl–Co(III) dissociation | $k_{dis,ben}$ | $1.4 \times 10^{-3}$ s$^{-1}$ | Extrapolated from ref. 24 |
| Spontaneous decomposition | $k_{dec}$ | $1 \times 10^{-4}$ to $1 \times 10^{-6}$ s$^{-1}$ | Estimated |

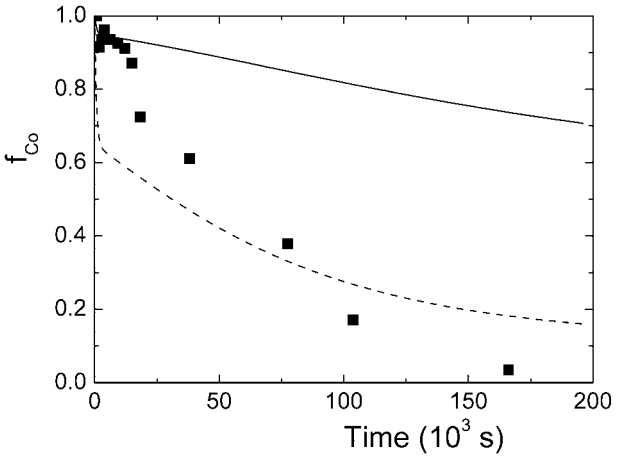


**Figure 11** Simulation results and experimental data for the CCT polymerization of MMA in toluene at 60°C. In the simulations deactivation is assumed to occur via transfer to solvent derived radicals. Rate constants are given in Tables II and III except for $k_{i,ben} = 8 \times 10^3$ L · mol$^{-1}$×s$^{-1}$ (solid curve); $k_{i,ben} = 8 \times 10^2$ L · mol$^{-1}$ · s$^{-1}$ (dashed curve).

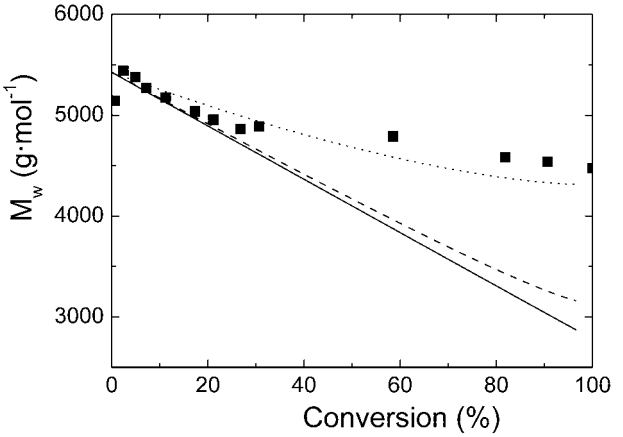


**Figure 13** Experimental and simulation results for the CCT polymerization of MMA in toluene at 60°C. Solid line: simulation according to the mechanism shown if Figure 2; dashed line: similar including macromonomer reinitiation with $k_{macro} = 1 \times 10^3$ L · mol$^{-1}$×s$^{-1}$; dotted line: similar including macromonomer reinitiation with $k_{macro} = 1 \times 10^4$ L · mol$^{-1}$ · s$^{-1}$.

### Additional growth of polymer chains

Polymer chains can be reinitiated in various ways. In CCT polymerization the growing radical chains can add to macromonomer resulting in transfer of the radical to the macromonomer. Furthermore, Cacioli et al.[33] have shown that copolymerization of methacrylate and macromer does not occur. Kowollik et al.[20] included the mechanism for transfer to macromer in their simulations and found hardly any effects on the MWD. This can be explained from the low concentration of macromer with respect to monomer in combination with a low chain transfer constant for macromer of about 0.2.[34]

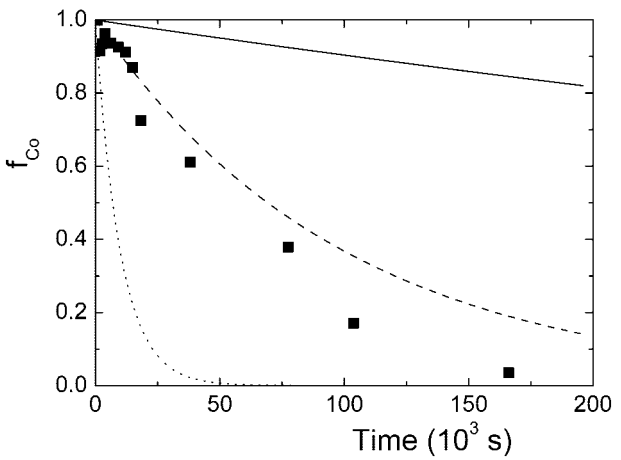


**Figure 12** Simulation results and experimental data for the CCT polymerization of MMA in toluene at 60°C. In the simulations deactivation is assumed to occur spontaneously. Rate constants are given in Table II except for $k_{dec} = 1 \times 10^{-6}$ s$^{-1}$ (solid curve); $k_{dec} = 1 \times 10^{-5}$ s$^{-1}$ (dashed curve); $k_{dec} = 1 \times 10^{-4}$ s$^{-1}$ (dotted curve).

A second possibility for additional growth of polymer chains is intermolecular chain transfer to polymer. For PMMA, chain transfer to polymer mainly occurs to the double bond originating from disproportionation.[35] This is a process analogous to chain transfer to macromonomer. As no reports on chain transfer to the polymer backbone were found, it is assumed to be negligible for MMA. A third option is reinitiation of macromonomer by cobalt hydride as suggested by Gridnev.[36] In Figure 13 the results are shown for simulations incorporating macromonomer reinitiation. The macromonomer reinitiation rate constant $k_{macro}$ is set at $1 \times 10^3$ L · mol$^{-1}$ · s$^{-1}$, equal to reinitiation of monomer and at $1 \times 10^4$ L · mol$^{-1}$ · s$^{-1}$, which is an order of magnitude larger. In the latter case a quite reasonable fit with the experimentally observed values of $M_w$ is obtained. However, there is no reason to expect reinitiation of macromonomer to proceed that much faster than reinitiation of monomer. Furthermore, macromer reinitiation can not occur in our system only. If it would occur, the experimental decrease in $M_w$ observed by Kowollik et al.[20] would have been smaller as well.

In the previous three sections some possible mechanisms have been discussed that may explain the evolution of molecular weight during a high conversion catalytic chain transfer polymerization. Though it is hard to pinpoint the right mechanism or mechanisms, some can be excluded or described as unlikely. Changes in intrinsic catalyst activity due to changes in composition or viscosity do not seem to play an important role. Additional growth of macromonomer

**TABLE IV**
**Experimental Results for the High Conversion CCT Polymerization of MMA in Bulk and Toluene at 60°C**

| Exp. | $w_{MMA}$ (—) | [CoBF] ($10^{-6}$ mol · $L^{-1}$) | $-\Delta M_w/M_w$ [a] (—) | [P•] ($10^{-8}$ mol · $L^{-1}$) | $C_T$ ($10^3$ —) |
|---|---|---|---|---|---|
| I | 1 | 9.1 | 0.17 | 2.3 | 40.8 |
| II | 0.42 | 3.0 | 0.18 | 2.7 | 46.1 |
| III | 0.42 | 1.0 | 0.37 | 2.9 | 42.7 |
| IV | 0.17 | 1.0 | 0.45 | 2.5 | 43.7 |

[a] Fractional decrease in $M_w$ over the complete conversion range.

can also be excluded, as this would contradict the experimental results of Kowollik et al.,[20] although in principle a model including reinitiation of macromonomer by cobalt hydride could explain the experimental observations reported in this work. Deactivation of cobalt(II) by solvent-derived radicals is unlikely as well, but it may occur in other solvents. This leaves decomposition of the Co(II) complex to be most probably responsible for the fact that the decrease in molecular weight with conversion is less than expected. So far, it is not clear what induces this decomposition.

### Effects of catalyst and solvent concentration

Two additional experiments were carried out to see whether the catalyst concentration and the solvent concentration affect the previous experimental observations. For comparison, the experimental data for the previous and the present experiments are gathered in Table IV.

The chain transfer coefficients for all experiments, determined from the second sample, are similar. The evolution of $M_w$ with conversion for experiments II–IV is shown in Figure 14. Although the fractional decrease in $M_w$ in percentage terms over the complete conversion range in experiments III and IV approximates the theoretical predictions of Kowollik et al., [20] the experimentally observed decrease predominantly occurs during the first stage of the polymerization, whereas theory predicts a nearly linear decrease (see Fig. 7).

The radical concentrations are all in the same range. Although the molecular weights for experiments II and III differ by a factor of 3, the radical concentrations differ only 7%, which is somewhat less than predicted by a combination of eq. (8),

$$[P^\bullet] = \left(\frac{fk_d[I]}{\langle k_t \rangle}\right)^{1/2} \tag{8}$$

and the following expression,

$$\langle k_t \rangle \sim P_n^{-a} \tag{9}$$

in which the average termination rate coefficient is related to the number average degree of polymerization and some coefficient $\alpha$. Suddaby et al.[36] and Kukulj et al.[16] predict values in the range 0.12 to 0.19 for $\alpha$, resulting in about a 15 % decrease in $M_w$. Heuts et al.[17] recently showed an even larger increase in radical concentration. However, the experiments of Heuts et al.[17] were carried out at catalyst concentrations resulting in polymers having $M_w$s less than one thousand, which may very well result in a change in the chain-length dependence of $\langle k_t \rangle$ with respect to the chain-length dependence of $\langle k_t \rangle$ for higher molecular weight polymers.[38]

The changes in the fraction of active cobalt(II) calculated according to eq. (7) are shown in Figure 15. The first aspect to be noticed is the 40% increase in active CoBF during the first 7% of conversion in experiment IV, the one having the lower monomer content. It is unlikely that this increase can be attributed to scatter only. If the chain transfer coefficient would be calculated from the fourth point in stead of the second, this would give a value around $59 \times 10^3$, which is in agreement with the results for low conversion polymerizations at high toluene concentrations as shown

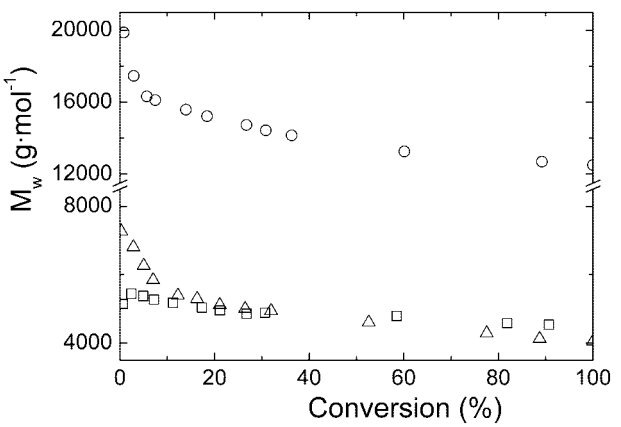


**Figure 14** The evolution of $M_w$ with conversion in the CCT polymerization of MMA in toluene at 60°C. Squares: experiment II, $w_{MMA}$ = 0.419, [CoBF] = $3.0 \times 10^{-6}$ mol · $L^{-1}$; circles: experiment III, $w_{MMA}$ = 0.419, [CoBF] = $1.0 \times 10^{-6}$ mol · $L^{-1}$; triangles: exp. IV, $w_{MMA}$ = 0.170, [CoBF] = $1.0 \times 10^{-6}$ mol · $L^{-1}$.

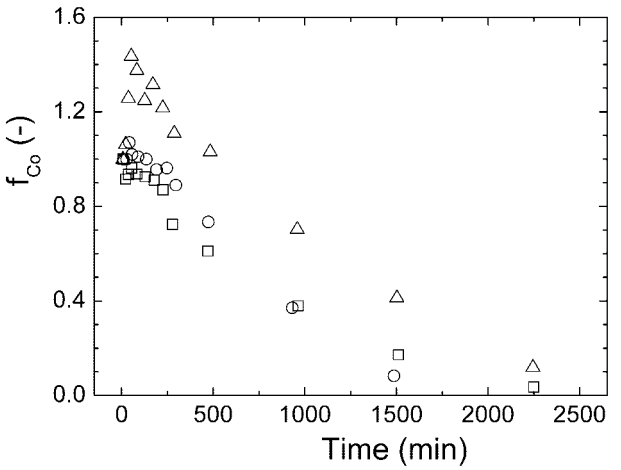


**Figure 15** Changes in the fraction of active catalyst in time for the CCT polymerization of MMA in toluene at 60°C. Squares: experiment II, $w_{MMA} = 0.419$, [CoBF] = $3.0 \times 10^{-6}$ mol · $L^{-1}$; circles: experiment III, $w_{MMA} = 0.419$, [CoBF] = $1.0 \times 10^{-6}$ mol · $L^{-1}$; triangles: experiment IV, $w_{MMA} = 0.170$, [CoBF] = $1.0 \times 10^{-6}$ mol · $L^{-1}$.

in a previous article,[29] although conversions were in between 2.4 and 3.6% in the latter case. The origin of the increase in $C_T$ at high concentrations of toluene, however, remains unclear.

In experiment IV, the fraction of active cobalt (II) starts decreasing after it has reached its peak after one hour. In experiments II and III, during the first 4–5 h of polymerization the fraction of active catalyst decreases only slowly after which a faster decomposition or deactivation sets in. In experiment III, in which the highest molecular weights are produced, the fastest deactivation also occurs. For longer reaction times the radical concentration in experiment III, determined from the slope of a first-order kinetic plot, increases with time. As can be seen in eq. (8), an increase in radical concentration may very well originate from a decrease in $\langle k_t \rangle$. A decrease in $\langle k_t \rangle$ is more likely to be observed in experiment III than in experiments II and IV, as the $M_w$ in experiment III is a factor of 3 larger than in the other experiments. This results in a stronger increase in viscosity in experiment III and thus a larger decrease in $\langle k_t \rangle$ with respect to experiments II and IV. When $\langle k_t \rangle$ is controlled by diffusion, depending on conversion and molecular weight, $k_{tr}$ may also become partially diffusion controlled. In the calculation of $f_{Co}$ no distinction can be made between a decrease in $C_T$ and a decrease in catalyst concentration. Therefore, a decrease in $k_{tr}$ would appear as enhanced deactivation. The fact that it is not possible to distinguish between changes in $C_T$ and [Co(II)] further complicates analysis. Disregarding all complications, calculating a first order deactivation rate constant over the part where faster deactivation or decomposition takes place would yield $k_{dec} = 1.4 - 2.5 \times 10^{-5}$ $s^{-1}$ for the experimental conditions used in these experiments. This corresponds to a half-life around 10 h at 60°C, which explains why this deactivation is not observed in short, low conversion, experiments. Unfortunately these experiments only show more complicating features and give no clear information about the origin of the effects, whether it is in solvent or monomer purity, in catalyst concentration or any other aspect of the experimental design. Although Kowollik and Davis[20] recently showed that, under presumably well-chosen conditions, the decrease in $M_w$ predicted theoretically may be achieved experimentally, the question still remains what causes the deviations observed in the present work and in the work reported by other authors. Further research is required to resolve these problems.

### The effects of acid and peroxides on catalyst deactivation

In previous work[39] it was shown that, to our surprise, both BPO at a concentration of $1 \times 10^{-3}$mol · $L^{-1}$ and acetic acid at a concentration of 1 mol · $L^{-1}$ do not affect the CCT polymerization of MMA at low conversions in contrast to literature reports.[40–44] Therefore, it was decided to perform a set of high conversion polymerizations with benzoyl peroxide and acetic acid as additives to see the effects of longer reaction times.

For both benzoyl peroxide and acetic acid two polymerizations were carried out at different additive concentrations. All experiments were performed at $w_{MMA} = 0.42$ and [CoBF] = $3.0 \times 10^{-6}$ mol · $L^{-1}$. In Table V the other experimental conditions and some results are given. The radical concentrations are determined from the slope in the first 5–6 h of a first-order kinetic plot. The chain transfer coefficients are ob-

**TABLE V**
**Experimental Data and Results for the CCT Polymerization of MMA in Toluene at 60°C**

| Exp. | Additive | [Add.] (mol · $L^{-1}$) | [P•] ($10^{-8}$ mol · $L^{-1}$) | $C_T$ ($10^3$ —) | $M_w$ at end ($10^3$ g · $mol^{-1}$) |
|---|---|---|---|---|---|
| V | HAc | 0.10 | 2.6 | 43.7 | 7.1 |
| VI | HAc | 1.0 | 2.9 | 51.6 | 15.7 |
| VII | BPO | $1.0 \times 10^{-3}$ | 2.9 | 39.2 | 18.1 |
| VIII | BPO | $4.0 \times 10^{-3}$ | 3.8 | 19.3 | 79.6 |

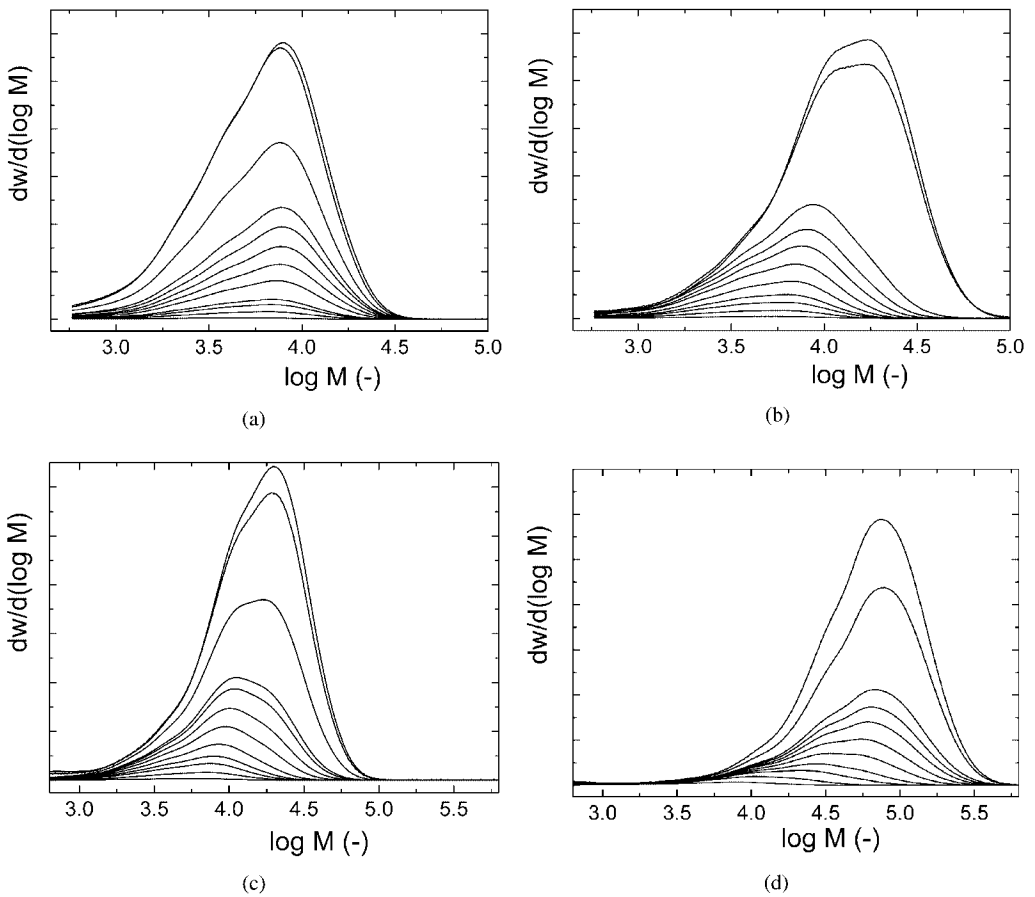


**Figure 16** Evolution of MWD with conversion in the CCT polymerization of MMA in toluene at 60°C in the presence of acetic acid or benzoyl peroxide at $w_{MMA} = 0.419$ and [CoBF] = $3.0 \times 10^{-6}$ mol · $L^{-1}$. (a) [HAc] = 0.1 mol · $L^{-1}$, conversion 0.5–94.9%; (b) [HAc] = 1.0 mol · $L^{-1}$, conversion 0.9–100%; (c) [BPO] = $1 \times 10^{-3}$ mol · $L^{-1}$, conversion 0.6–100%; (d) [BPO] = $4 \times 10^{-3}$ mol · $L^{-1}$, conversion 1.2 –100 %. The areas under the MWDs are proportional to conversion.

tained from the second sample as explained above. The evolution of the molecular weight distributions with conversion is shown in Figure 16(a–d).

Table V and Figure 16 clearly demonstrate the effect of the additives. In all polymerizations $M_w$ increases with conversion, whereas a decrease in $M_w$ in absence of additives was observed. The $M_w$ at the end of polymerization for experiment II, under similar conditions without additives, was $4.5 \times 10^3$ g · $mol^{-1}$. The increase in $M_w$ with conversion is caused by deactivation of the Co(II) species, which, in contrast to the experiments up to low conversions, is clearly observed here. As can be seen in Figures 16 c and d, especially for BPO, the increase in $M_w$ and thus the deactivation is very rapid, which even results in a decreased $C_T$ as determined from the second sample. The rates of polymerization are quite similar to those in the previous experiments except for the experiment at [BPO] = $4 \times 10^{-3}$ mol · $L^{-1}$. The increased rate for the experiment at [BPO] = $4 \times 10^{-3}$ mol · $L^{-1}$ is due both to enhanced radical formation and to a decreased termination rate constant. In addition, all four experiments show an increased polymerization rate at higher conversions due to an increase in reaction mixture viscosity, resulting in a decrease in $\langle k_t \rangle$ and thus an increase in radical concentration.

### Mechanism and modeling for BPO-induced deactivation

The trends in cobalt(II) deactivation can be found in Figure 17 for experiments with BPO. An attempt was made to model the polymerizations using Predici. The same set of reactions and rate constants as presented in Figure 3 and Table II is used. Additional rate constants for reactions involving BPO are taken from the literature[45] or are estimated and both are collected in Table VI. Transfer to BPO results in termination of a growing polymer chain and in the formation of one benzoyloxy radical, and must therefore be taken into account as well. It must be realized that next to deactivation induced by either of these species, deactivation observed in absence of any additives will occur simultaneously. This is accounted for by a first-order decomposition reaction as defined in Table VI. The simulation results are shown in Figure 17 as well.

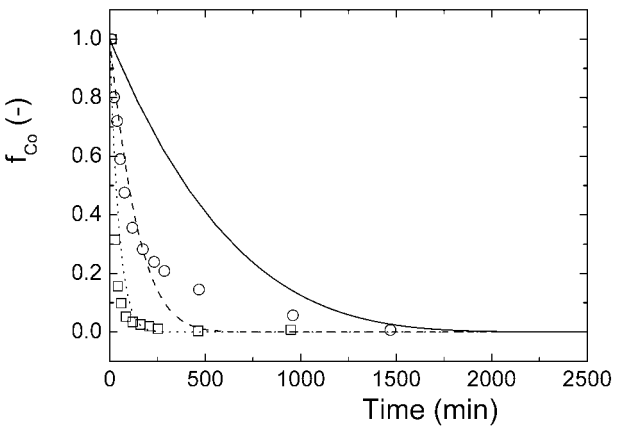


**Figure 17** The evolution of the fraction of cobalt(II) in the CCT polymerization of MMA in toluene at 60°C in the presence of benzoyl peroxide. Experimental: circles: $1.0 \times 10^{-3}M$ BPO; squares: $4.0 \times 10^{-3}M$ BPO. Simulations: solid curve: $k_{com,B}/k_{i,B} = 10^3$; dashed curve: $k_{com,B}/k_{i,B} = 10^3$ and $1 \times 10^{-3}M$ BPO; dotted curve: $k_{com,B}/k_{i,B} = 5 \times 10^4$ and $4 \times 10^{-3}M$ BPO.

Gridnev[44] used a different approach to model deactivation. He considered a direct reaction between a hydrogen-bridged cobaloxime and benzoyl peroxide with a reaction rate constant of about 10 L mol $\cdot^{-1} \cdot$ $s^{-1}$. For the conditions employed in this study this would result in a half-life of the CoBF of less than 2 min. As the observed deactivation is clearly slower, this step is not taken into account here.

The solid curve in Figure 17 results from the simulations using the rate constants in Table VI. According to the simulations, deactivation is not expected to be as fast as observed experimentally. The slower deactivation stemming from the simulations can be understood when the probability of a benzoyloxy radical, $B^{\bullet}$, combining with CoBF is calculated according to

$$\frac{k_{com,B}[Co(II)][B^{\bullet}]}{k_{i,B}[MMA][B^{\bullet}] + k_{com,B}[Co(II)][B^{\bullet}]} = 7.5 \times 10^{-4} \quad (10)$$

which means that less than 1 in every one thousand benzoyloxy radicals will combine with CoBF.

Several possible explanations can be given for the discrepancy between experimentally observed deactivation and deactivation occurring in simulations. First of all, one or more rate constants may have been incorrectly estimated or determined. The reaction steps affecting the deactivation rate most are combination and initiation. The combination rate constant $k_{com,B}$ seems to be well estimated for a radical–radical combination, but could be underestimated in view of the high reactivity of benzoyloxy radicals. The initiation rate constant $k_{i,B}$ is not expected to be overestimated by more than one order of magnitude, as it is based on several literature resources. To obtain a better agreement with the experimental data a change in the ratio of combination and initiation rate constants from $1 \times 10^3$ to $5 \times 10^4$ is required. Such a change is quite large, though not impossible. The simulation results for these input data are shown as the dashed and dotted curves for [BPO] is $1 \times 10^{-3}$ mol $\cdot$ $L^{-1}$ and $4 \times 10^{-3}$ mol $\cdot$ $L^{-1}$, respectively.

A second explanation for the discrepancy between the initial simulations and experimental results could also be the occurrence of contaminants in BPO, as it was not purified before use. A similar effect of impurities was observed before for AIBN as described by Vollmerhaus et al.[31] These contaminants should in that case be orders of magnitude more reactive towards CoBF than the benzoyloxy radicals, which is unlikely, but cannot be excluded at this point.

If deactivation occurs via combination of benzoyloxy radicals and CoBF, then the peroxide induced deactivation rate equals

$$-\frac{d[CoBF]}{dt} = k_{com,B}[CoBF][B^{\bullet}] \quad (11)$$

Assuming a steady state in benzoyloxy radicals, its concentration can be calculated from

$$\frac{d[B^{\bullet}]}{dt} = 0 = 2k_{d,B}[BPO] - k_{i,B}[B^{\bullet}][MMA] - k_{com,B}[B^{\bullet}][CoBF] - k_t[B^{\bullet}][P^{\bullet}] \quad (12)$$

In expression (12) the termination term can be neglected compared to the other terms, as the concentration of polymeric radicals is very small with respect to

**TABLE VI**
**Additional Rate Coefficients Involved in BPO- or HAc-induced Deactivation**

| Description | Rate constant | Value | Reference/remarks |
|---|---|---|---|
| Decomposition of BPO | $k_{d/BPO}$ | $2.8 \times 10^{-6}$ $s^{-1}$ | Ref. 45 |
| Initiation of MMA by benzoyloxy radical | $k_{i,B}$ | $1 \times 10^6$ L $\cdot$ $mol^{-1} \cdot s^{-1}$ | Lower limit estimated from ref. 34 |
| Transfer to BPO | $k_{tr,BPO}$ | 16.7 L $\cdot$ $mol^{-1} \cdot s^{-1}$ | Ref. 32 |
| Combination of benzoyloxy radical and CoBF | $k_{com,B}$ | $1 \times 10^9$ L $\cdot$ $mol^{-1} \cdot s^{-1}$ | Estimated |
| Spontaneous CoBF decomposition | $k_{dec}$ | $2 \times 10^{-5}$ $s^{-1}$ | Calculated from exp. II |

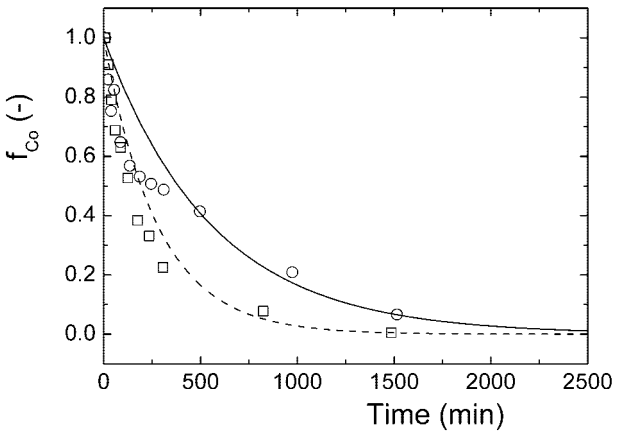


**Figure 18** The evolution of the fraction of cobalt(II) in the CCT polymerization of MMA in toluene at 60°C in the presence of acetic acid. Experimental: circles: 0.10*M* HAc; squares: 1.0*M* HAc. Simulations: solid curve: $k_{dec,H} = 1 \times 10^5\ s^{-1}$; $k_{dec,H} = 4 \times 10^{-5}\ s^{-1}$.

monomer concentration, which results in a linear dependence of the benzoyloxy radical concentration on benzoyl peroxide concentration. Combining this with eq. (11) gives

$$-\frac{d[\mathrm{CoBF}]}{dt} = \frac{2k_{com,B}k_{d,B}[\mathrm{CoBF}][\mathrm{BPO}]}{k_{i,B}[\mathrm{MMA}] + k_{com,B}[\mathrm{CoBF}]} \quad (13)$$

For experiments V and VI this would mean a factor of 4 difference in initial deactivation rate. This compares well with the 20 and 70% deactivations found experimentally for the second sample as shown in Figure 17 and supports that deactivation indeed occurs via benzoyloxy radicals.

### Mechanism and modeling for HAc-induced deactivation

The experimental trends in cobalt(II) deactivation for CCT polymerizations in the presence of HAc are presented in Figure 18. In order to describe these polymerizations, Predici simulations were performed. The same standard set of reaction steps and rate constants as presented above is used. Instead of the additional reaction steps for BPO, only two additional reactions are considered, viz. spontaneous decomposition of CoBF with a rate constant $k_{dec} = 2 \times 10^{-5}\ s^{-1}$ and acid-induced decomposition with a rate constant $k_{decH} = 10^{-4} - 10^{-6}\ s^{-1}$. The simulation results for the experiments in which acetic acid has been added to the reaction mixture are presented in Figure 18 as well. The rate constants for acid-induced decomposition were not obtained from a statistical fitting procedure, but determined by trial and error to show reasonable agreement between experimental data and simulations, as at this stage our main interest is in describing the main trends. It is clear that with the rate constants chosen from the range $10^{-4} - 10^{-6}\ s^{-1}$ the experimental data can be in good agreement with the simulations. However, it is important to see whether it is possible to relate the rate constants for decomposition $1 \times 10^{-5}\ s^{-1}$ and $4 \times 10^{-5}\ s^{-1}$ to their respective acetic acid concentrations 0.10 and 1.0*M*. Similar to Bakac and Espenson[24] the overall decomposition of CoBF is described as a first-order process, but in order to relate rate constants to acid concentrations, a more complete description of the actual mechanism is needed. It is not unlikely that an acid–base equilibrium sets in between CoBF and acetic acid and that protonated CoBF (CoBF-$H^+$) can subsequently decompose (see Fig. 19). A similar mechanism was suggested by Gridnev for the less stable proton-bridged cobaloximes.[44] As CoBF is expected to be a very weak base, the acid–base equilibrium will be on the left-hand side.

The acid- induced decomposition rate can be expressed as

$$-\frac{d[\mathrm{CoBF}]}{dt} = k'_{decH}[\mathrm{CoBF} - \mathrm{H}^+] \quad (14)$$

Using a charge balance and mass balances for both CoBF and acetic acid and the expression for the acid–base equilibrium shown in Figure 19, it can be derived that the decomposition rate equals

$$-\frac{d[\mathrm{CoBF}]}{dt} = k'_{decH}K_H^{1/2}[\mathrm{CoBF}]_0^{1/2}[\mathrm{HAc}]_0^{1/2} \quad (15)$$

in which $[CoBF]_0$ and $[HAc]_0$ are the initial concentrations of CoBF and HAc. This expression is valid provided that only a small part of CoBF is protonated. According to this equation a factor of 10 change in acid concentration results in a factor of $10^{1/2} = 3.16$ change in decomposition rate. This is in good agreement with the factor of 4 change in the estimated overall rate constants for acid induced decomposition.

The trends and expressions shown here may also be useful in modeling CCT (co)polymerization with methacrylic acid, in which CoBF decomposition is known to take place.[41]

## CONCLUSIONS

In this work the evolution of molecular weight in the high-conversion CCT polymerization of MMA in tol-

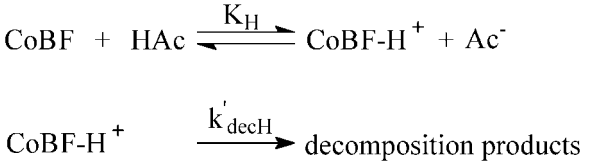


**Figure 19** Mechanism for acid-induced decomposition of CoBF.

uene has been investigated both by experiments and simulations. In contrast to most other reports in literature, recent results reported by Kowollik et al.[20] demonstrating that under appropriate conditions the molecular weight decreases with conversion, have now been confirmed. Simulations predict a nearly linear decrease in $M_w$ if the CoBF concentration remains unchanged. However, in most experiments this decrease was less than expected or was reached in a nonlinear way.

Simulations on various mechanisms that may explain experimental results have been performed. In general, mechanisms based on changes in intrinsic catalyst activity or on additional growth of polymer chains can be excluded. Only in experiments were a strong increase in $M_w$ is found, diffusion control may result in an additional decrease in catalyst activity leading to a further increase in $M_w$. Simulations demonstrated that catalyst deactivation via solvent-derived radicals is unlikely as well. Thus, in spite of purification of all reaction components and performing the reactions inside a glovebox, catalyst deactivation is the most likely cause for the discrepancy between experimental and theoretical results. The origin of the deactivation reaction pathway remains unclear.

Under the conditions of the experiments described in this chapter a half-life for CoBF of about 10 h at 60°C was determined. This is in agreement with the results from short, low-conversion experiments where, under similar conditions, no deactivation is observed. Finally, it can be concluded that both acetic acid and benzoyl peroxide enhance catalyst deactivation. For benzoyl peroxide the initial deactivation rate is proportional to the benzoyl peroxide concentration. For acetic acid, on the other hand, the deactivation rate is proportional to the square root of the acid concentration. This relation can also be useful in predictions of CoBF activity in the polymerization of acidic monomers.

## References


1. Enikolopyan, N. S.; Smirnov, B. R.; Ponomarev, G.V.; Belgovskii, I. M. J Polym Sci, Polym Chem Ed 1981, 19, 879.
2. Burczyk, A. F.; O'Driscoll, K. F.; Rempel, G. L. J Polym Sci, Polym Chem Ed 1984, 22, 3255.
3. Smirnov, B. R.; Plotnikov, V. D.; Ozerkovskii, B. B.; Roshchupkin, V. P. Enikolopyan, N. S. Polym Sci USSR (Engl Transl) 1981, 23, 2807.
4. Heuts, J. P. A.; Kukulj, D.; Forster, D. J.; Davis, T. P. Macromolecules 1998, 31, 2894.
5. Kukulj, D.; Heuts, J. P. A.; Davis, T. P. Macromolecules 1998, 31, 6034.
6. Kukulj, D.; Davis, T. P.; Suddaby, K. G.; Haddleton, D. M.; Gilbert, R. G. J Polym Sci, Polym Chem Ed 1997, 35, 859.
7. Pierik, B.; Masclee, D.; van Herk, A. Macromol Symp 2001, 165, 19.
8. Davis, T. P.; Haddleton, D. M.; Richards, S. N. J Macromol Sci, Rev Macromol Chem Phys1994, C34, 23.
9. Davis, T. P.; Kukulj, D.; Haddleton, D. M.; Maloney, D. R. Trends Polym Sci 1995, 3, 365.
10. Gridnev, A. A.; Ittel, S. D. Chem Rev 2001, 101, 3611.
11. Heuts, J. P. A.; Roberts, G. E.; Biasutti, J. D. Aust J Chem 2002, 55, 381.
12. Suddaby, K. G.; Amin Sanayei, R. A.; Rudin, A.; O' Driscoll, K. F. J Appl Polym Sci 1991, 43, 1565.
13. Grady, M. C. Ph.D. thesis, ETH Zurich, Zurich, 1996.
14. Abbey, K. J.; Carlson, G. M.; Masola, M. J.; Trumbo, D. Polym Mater Sci Eng 1986, 55, 235.
15. Yamada, B.; Tagashira, S.; Aoki, S. J Polym Sci, Part A: Polym Chem 1994, 32, 2745. 16. Kukulj, D.; Davis, T. P. Macromol Chem Phys 1998, 199, 1697.
17. Heuts, J. P. A.; Forster, D. J.; Davis, T. P.; Yamada, B.; Yamazoe, H.; Azukizawa, M. Macromolecules 1999, 32, 2511.
18. Heuts, J. P. A.; Forster, D. J.; Davis, T. P. Macromol Rapid Commun 1999, 20, 299.
19. Heuts, J. P. A.; Forster, D. J.; Davis, T. P. In Transition Metal Catalysis in Macromolecular Design; Boffa, L. S., Novak, B. M., Eds.; ACS Symposium Series; American Chemical Society: Washington, DC, 2000; Vol 760, p 254.
20. Kowollik, C.; Davis, T. P. J Polym Sci, Part: A Polym Chem 2000, 38, 3303.
21. Muratore, L. M.; Heuts, J. P. A.; Davis, T. P. Macromol Chem Phys 2000, 201, 985.
22. Heuts, J. P. A.; Muratore, L. M.; Davis, T. P. Macromol Chem Phys 2000, 201, 2780.
23. Pangborn, A. B.; Giardello, M. A.; Grubbs, R. H.; Rosen, R. K.; Timmers, F. J. Organometallics 1996, 15, 1518.
24. Bakac, A.; Espenson, J. H. J Am Chem Soc 1984, 106, 5197.
25. Hutchinson, R. A.; Paquet, D. A.; McMinn, J. H.; Beuermann, S.; Fuller, R. E.; Jackson, Dechema, C. Monographs 1995, 131, 467.
26. Walbiner, M.; Wu, J. Q.; Fischer, H. Helv Chim Acta 1995, 78, 810.
27. van Herk, A. M. Macromol Theory Simul 2000, 9, 433.
28. Kowollik, C. Ph.D. thesis, University of Göttingen, Cuvillier Verlag, Göttingen, 1999.
29. Pierik, S. C. J.; Vollmerhaus, R.; van Herk, A. M. Macromol Chem Phys, 2003, 204, 1090.
30. Roberts, G. E.; Davis, T. P.; Heuts, J. P. A.; Russell, G. T. J Polym Sci, Part A: Polym Chem 2002, 40, 782.
31. Vollmerhaus, R.; Pierik, S. C. J.; van Herk, A. M. Macromol Symp 2001, 165, 123.
32. Ueda, A.; Nagai, S. In Polymer Handbook, 4th ed.; Brandrup, J., Immergut, E. H., Grulke, E. A., Eds.; John Wiley & Sons: New York, 1999; p II/97.
33. Cacioli, P.; Hawthorne, D. G.; Laslett, R. L.; Rizzardo, E.; Solomon, D. H. J Macromol Sci, Chem 1986, A23, 839.
34. Moad, C. L.; Moad, G.; Rizzardo, E.; Thang, S. H. Macromolecules 1996, 29, 7717.
35. Moad, G. ; Solomon, D. H. The Chemistry of Free Radical Polymerization, 1st ed.; Pergamon: Oxford, 1995.
36. Gridnev, A. A. J Polym Sci, Part A: Polym Chem 2000, 38, 1753.
37. Suddaby, K. G.; Maloney, D. R.; Haddleton, D. M. Macromolecules 1997, 30, 702.
38. de Kock, J. B. L. Ph.D. thesis, Eindhoven University of Technology, Eindhoven, 1999.
39. Pierik, S. C. J.; Vollmerhaus, R.; van Herk, A. M.; German, A. L. Macromol Symp 2002, 182, 43.
40. Suddaby, K. G.; Haddleton, D. M.; Hastings, J. J.; Richards, S. N.; O'Donnell, J. P. Macromolecules 1996, 29, 8083.
41. Haddleton, D. M.; Kelly, E. J.; Kukulj, D.; Morsley, S. M.; Steward, A. G. Polym Prep (ACS) 1999, 40(1), 381.
42. Karmilova, L. V.; Ponomarev, G. V.; Smirnov, B. R.; Belgovskii, I. M. Russian Chem Rev 1984, 53, 132.
43. Gridnev, A. A. Polym Sci USSR 1989, 31, 2369.
44. Gridnev, A. A. Polym J 1992, 24, 613.
45. Dixon, K. W. In Polymer Handbook, 4th ed.; Brandrup, J., Immergut, E. H., Grulke, E. A., Eds.; John Wiley & Sons: New York, 1999; p II/27.